Supplementary Material

The γ-MnO_2/NF mediated peroxymonosulfate activation for expeditious 2,4,6-trichlorophenol degradation: performance, pathways, and mechanism

Ranyun Xu[1,2], Qiaohui Shen[3], Lyujun Chen (✉)[4]

[1] School of Engineering, Hangzhou Normal University, Hangzhou 310018, China.

[2] Zhejiang Provincial Key Laboratory of Wetland Intelligent Monitoring and Ecological Restoration, Hangzhou 310018, China.

[3] Zhejiang Ecological and Environmental Monitoring Center, Hangzhou 310020, China.

[4] School of Environment, Tsinghua University, Beijing 100084, China.

List of Supporting Material

Figures

✉ Corresponding author
E-mail: chenlj@mail.tsinghua.edu.cn

Figure S8 Mass spectrums of of 2,4,6-TCP degradation intermediates

Tables

Table S1 List of reagents and materials

Table S2 Comparison of 2,4,6-TCP removal efficiency by different oxidation treatments

Table S3 Comparison of Mn leaching by different manganese oxide-based catalysts

Table S4 The observed degradation intermediates from the •OH/$SO_4^{\bullet-}$ oxidation of 2,4,6-TCP

Table S5 The acute/chronic toxicity levels of 2,4,6-TCP and its degradation intermediates

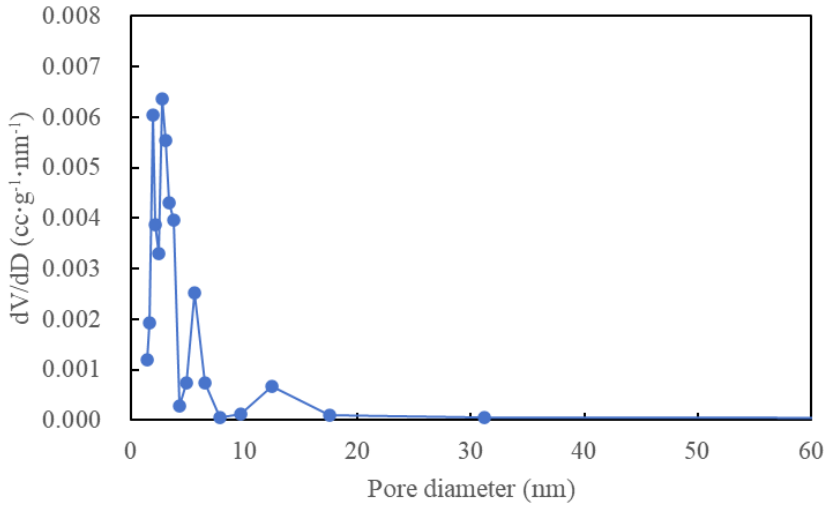

Figure S1 The pore size distribution of γ-MnO_2/NF

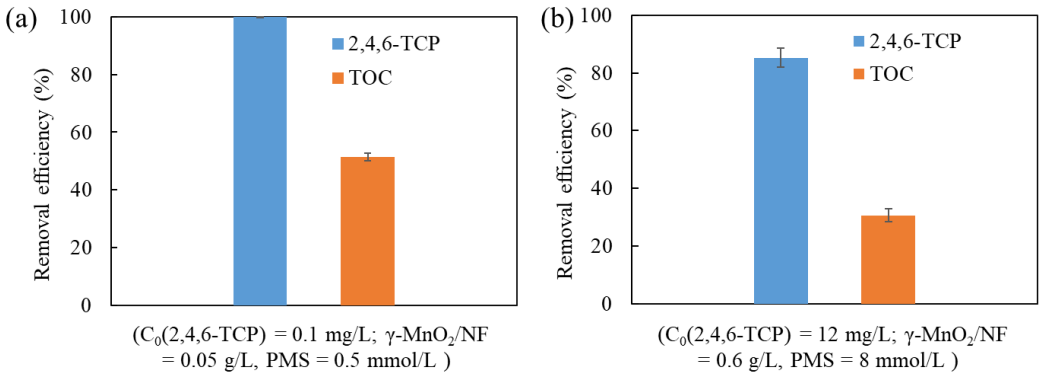

Figure S2 The treatment efficiency of γ-MnO_2/NF + PMS oxidation system for (a) environmental water and (b) industrial wastewater

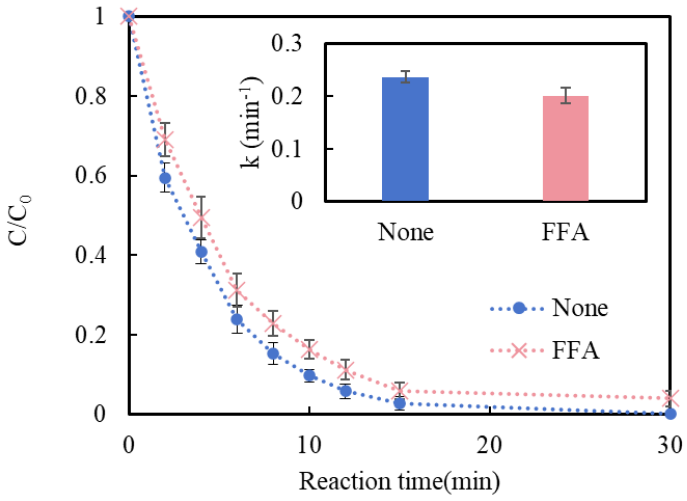

Figure S3 Effect of furfuryl alcohol (FFA) on 2,4,6-TCP degradation

(a) $H11_{abs}$ (b) $H12_{abs}$ (c) $H13_{abs}$

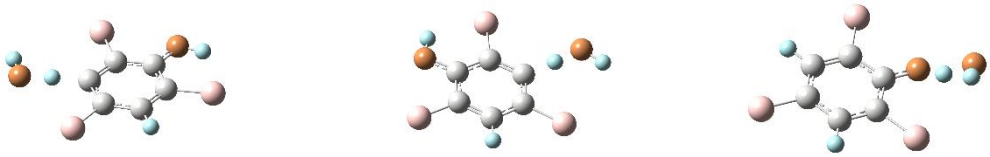

(d) $C1_{add}$ (e) $C2_{add}$ (f) $C3_{add}$

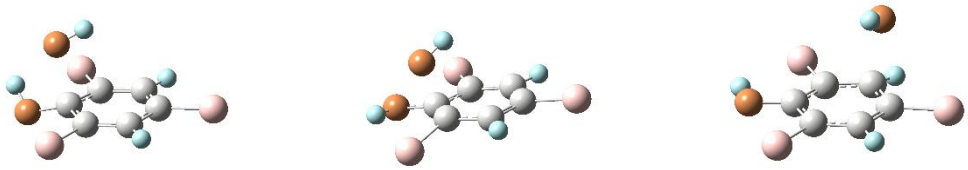

(g) $C4_{add}$ (h) $C5_{add}$ (i) $C6_{add}$

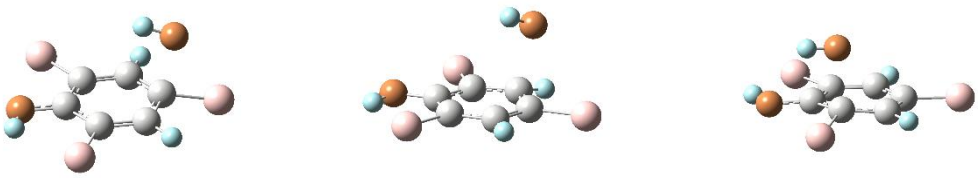

Figure S4 Model TS species structures for the reaction of 2,4,6-TCP and •OH via (a–c) HAA and (d–i) RAF pathways at M06–2X/6–31 + G** level of theory

(a) $H11_{abs}$ (b) $H12_{abs}$ (c) $H13_{abs}$

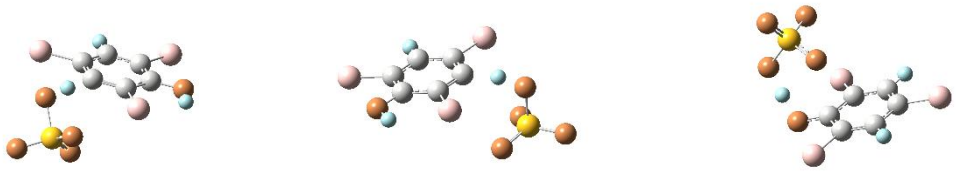

(d) $C1_{add}$ (e) $C2_{add}$ (f) $C3_{add}$

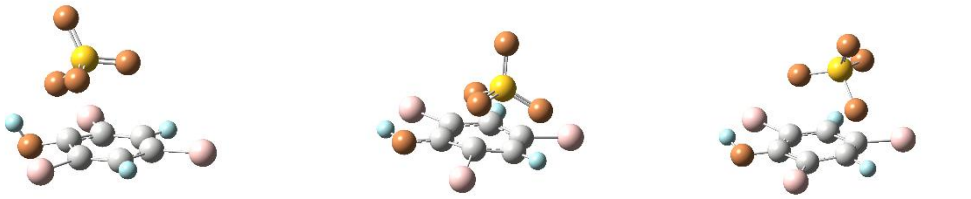

(g) $C4_{add}$ (h) $C5_{add}$ (i) $C6_{add}$

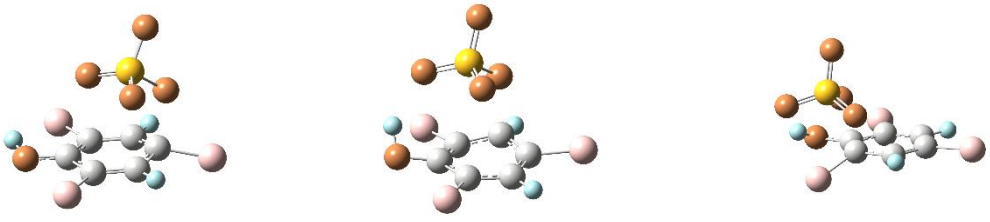

Figure S5 Model TS species structures for the reaction of 2,4,6-TCP and $SO_4^{\bullet-}$ via (a–c) HAA and (d–i) RAF pathways at M06–2X/6–31 + G** level of theory

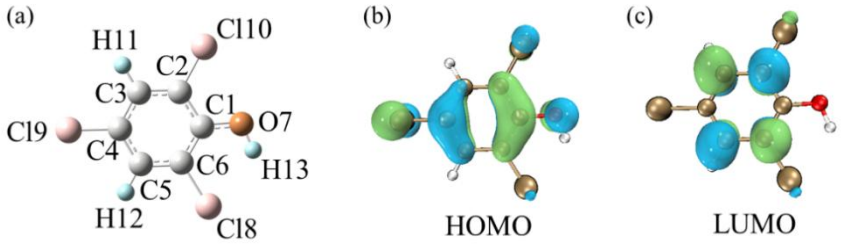

Figure S6 The (a) structure, (b) HOMO and (c) LUMO distribution of 2,4,6-TCP at SMD/M06-2X/6-31 ++ G** level of theory (The green and blue color refer to the positive and negative wave function)

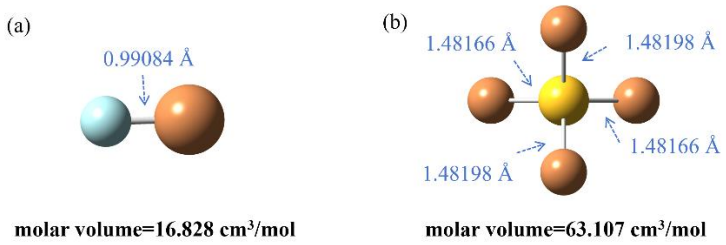

Figure S7 The bond length and molar volume of (a) •OH and (b) $SO_4^{\bullet -}$ at M06-2X/6-31 + G** level of theory

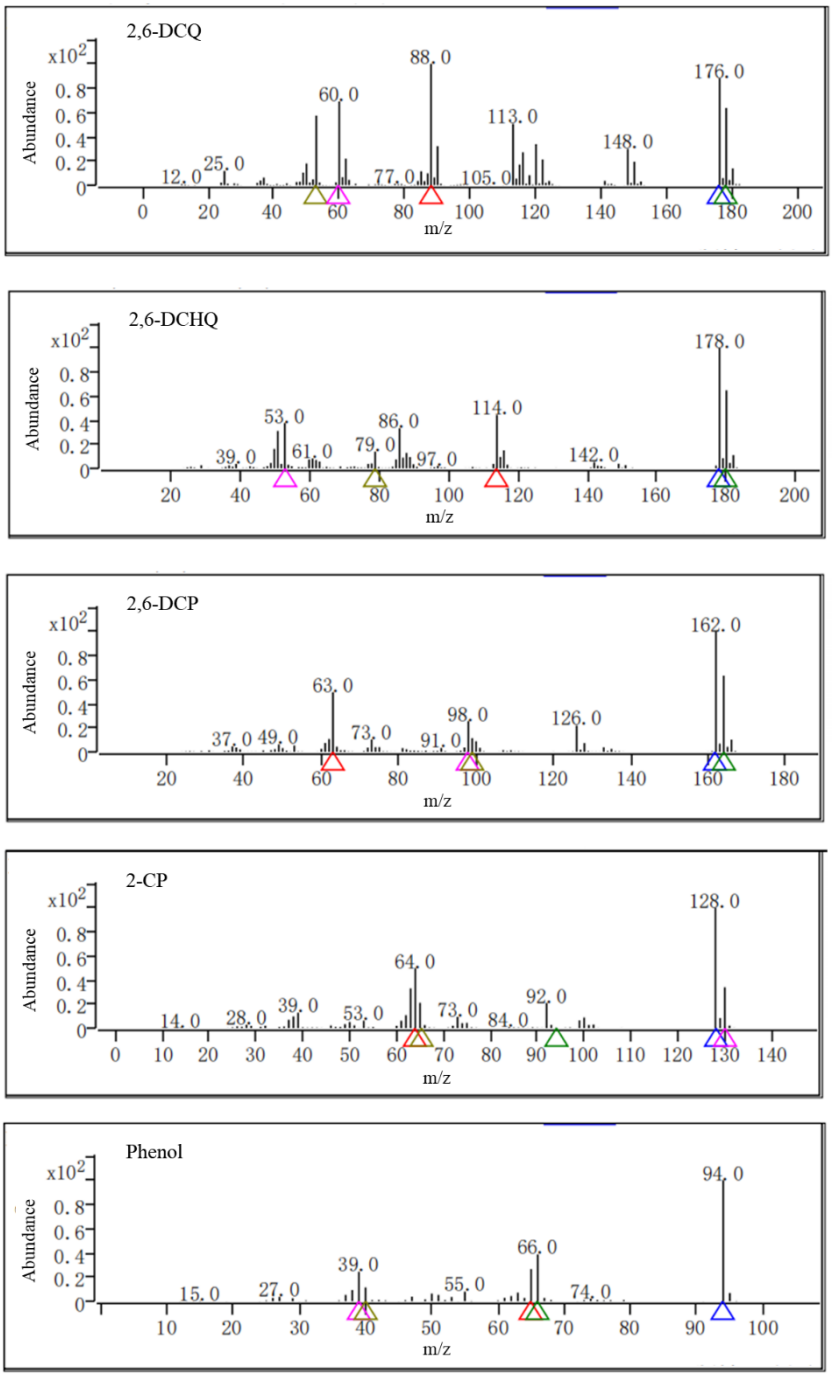

Figure S8 Mass spectrums of 2,4,6-TCP degradation intermediates

Table S1 List of reagents and materials

Reagent/Material	Purity	Supplier
Granular activated carbon	≥99.5%	Meryer, China
Nickel foam	≥99.5%	Goodfellow, the UK
Potassium permanganate	≥99.5%	Hushi, China

Manganese sulfate	99.99%	Innochem, China
Sodium sulphite	≥98%	Aladdin, China
Nitric acid	65-68%	Lanyi Chemical Product, China
Sulfuric acid	95%	Acros, China
Sodium hydroxide	≥96%	Innochem, China
Methanol	for HPLC, ≥99.9%	Fisher, China
Potassium chloride	≥99.99%	Innochem, China
Calcium chloride	96%	Innochem, China
Magnesium sulfate heptahydrate	≥99%	Aladdin, China
Magnesium chloride hexahydrate	98%	Innochem, China
Sodium bicarbonate	≥99.8%	Aladdin, China
Sodium nitrate	≥99%	Aladdin, China
Potassium phosphate monobasic	99.5%	Innochem, China
Disodium hydrogenphosphate 12& hydrate	99%	Innochem, China
Sodium chloride	≥99.8%	Aladdin, China
Glycerol	99%	Acmec, China
Yeast extract	BR	Aladdin, China
Tryptone	BR	Aladdin, China
2,4,6-Trichlorophenol	98%	Macklin, China
2,6-Dichlorophenol	99%	Macklin, China
2,4-Dichlorophenol	≥99.7%	Macklin, China
2-Chlorophenol	99%	Macklin, China
phenol	99.00%	Macklin, China
2,6-Dichloro-1,4-Dhenyldiol	99.4%%	CATO, China
2,6-Dichloro-1,4-Benzoquinone	98%	Macklin, China
Vibrio qinghaiensis sp. -Q67（Q67）	/	Research Center for Eco-Environmental Sciences, Chinese Academy of Sciences, China

Table S2 Comparison of 2,4,6-TCP removal efficiency by different oxidation treatments

Treatment system	Reaction time	Degradation efficiency (%)	kobs (min^{-1})	Reference

$CuO@g\text{-}C_3N_4$+PMS	25min	94	--	(Wang et al., 2024b)
Fe_3S_4+PMS	30min	17.89	--	(Li et al., 2022)
Fe_3S_4/BC+PMS	30min	67.79	--	
NMP_B+PDS	6 h	90.3	0.006	(Cui et al., 2024)
Fe-C+PMS	40 min	43	0.03	(Tang et al., 2025)
Fe-NC-0+PMS	40 min	69	0.06	
Fe-NC-1+PMS	40 min	99	0.17	
FeMnCN-700+PMS	30 min	94	0.083	(Xiong et al., 2022)
eMn@NG-4–700+PMS	30 min	97	0.148	
γ-MnO_2/NF+PMS	30 min	99	0.218	This study

Table S3 Comparison of Mn leaching by different manganese oxide-based catalysts

Qxidation system	Operation condition	Mn leaching (mg/L)	Reference
MnO_2+UV+PMS	PMS=1 mmol/L , MnO_2=0.25 g/L , pH = 4.0, T= 45 min	0.18–0.30	(Eslami et al., 2018)
MnO_2+PMS		0.19–0.27	
FeMn/GNs+PMS	PMS=0.65 mmol/L, FeMn/GNs =0.2 g/L, pH=3.5, T= 15 min	0.47	(Liu et al., 2023)
Co@α-MnO_2+PMS	Co@α-MnO_2=0.5 g/L, PMS=10 mmol/L, T=20 min	0.5	(Wang et al., 2024a)
IC-MnO_2+PMS	IC-MnO_2=0.2 g/L, PMS=0.65 mmol/L, pH=8.2, T=15 min	0.08–0.12	(Cheng et al., 2023)
S-CuMnO+PMS	S-CuMnO=0.07 g/L, PMS=0.8 mmol/L, T=30 min	2~18	(Li et al., 2021)

Table S4 The observed degradation intermediates from the •OH/$SO_4^{\bullet-}$ oxidation of 2,4,6-TCP

Compound	structure	Molecular formula	molecular weight	Precursor ion	Reference

				(g/mol)	(m/z)	
P1	2,6-DCQ	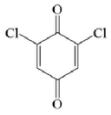	$C_6H_2Cl_2O_2$	176.98	176	(Ji et al., 2013)
P2	2,6-DCHQ	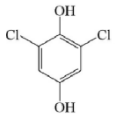	$C_6H_4Cl_2O_2$	179.00	178	(Ji et al., 2013)
P3	2,6-DCP	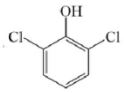	$C_6H_4Cl_2O$	163.00	162	(Xu et al., 2022)
P4	2-CP		C_6H_5ClO	128.55	128	(Yazdanbakhsh et al., 2018)
P5	Phenol		C_6H_6O	94.11	94	(Lebedev et al., 2018)

Table S5 The acute/chronic toxicity levels of 2,4,6-TCP and its degradation intermediates

Compound	Acute toxicity level (mg/L)			Chronic toxicity level (mg/L)		
	Fish LC50 (96h)	Daphnid LC50 (48h)	Green Algae EC50 (96h)	Fish ChV	Daphnid ChV	Green Algae ChV
2,4,6-TCP	2.72	2.27	0.25	0.31	0.32	0.76
2,6-DCQ	0.14	0.13	0.24	0.01	0.09	0.34
2,6-DCHQ	0.30	1.01	0.17	0.02	0.07	0.03
2,6-DCP	6.24	3.88	0.57	0.67	0.49	1.46
2-CP	13.66	6.35	1.21	1.37	0.71	2.67
Phenol	27.74	9.64	2.40	2.61	0.97	4.53

References

Cheng L, Bai J, Wei M, Zhao S, Xu A, Li X (2023). Carbon ink modified α-MnO2 as a peroxymonosulfate activator for enhanced degradation of organic pollutants via a direct electron transfer process. Colloids and Surfaces A: Physicochemical and Engineering Aspects, 658: 130772 doi:10.1016/j.colsurfa.2022.130772

Cui X, Hou D, Tang Y, Qie H, Xu R, Zhao P, Lin A, Liu M (2024). Natural magnetite as an efficient green catalyst boosting peroxydisulfate activation for pollutants degradation. Chemical Engineering Journal, 489: 151076 doi:10.1016/j.cej.2024.151076

Eslami A, Hashemi M, Ghanbari F (2018). Degradation of 4-chlorophenol using catalyzed peroxymonosulfate with nano-MnO2/UV irradiation: toxicity assessment and evaluation for industrial wastewater treatment. Journal of Cleaner Production, 195: 1389–1397 doi:10.1016/j.jclepro.2018.05.137

Ji H, Chang F, Hu X, Qin W, Shen J (2013). Photocatalytic degradation of 2,4,6-trichlorophenol over g-C3N4 under visible light irradiation. Chemical Engineering Journal, 218: 183–190 doi:10.1016/j.cej.2012.12.033

Lebedev A T, Polyakova O V, Mazur D M, Artaev V B, Canet I, Lallement A, Vaïtilingom M, Deguillaume L, Delort A M (2018). Detection of semi-volatile compounds in cloud waters by GC×GC-TOF-MS. Evidence of phenols and phthalates as priority pollutants. Environmental Pollution, 241: 616–625 doi:10.1016/j.envpol.2018.05.089

Li H, Li S, Jin L, Lu Z, Xiang M, Wang C, Wang W, Zhang J, Li C, Xie H (2022). Activation of peroxymonosulfate by magnetic Fe3S4/biochar composites for the efficient degradation of 2,4,6-trichlorophenol: synergistic effect and mechanism. Journal of Environmental Chemical Engineering, 10(1): 107085 doi:10.1016/j.jece.2021.107085

Li W, Wang Z, Liao H, Liu X, Zhou L, Lan Y, Zhang J (2021). Enhanced degradation of 2,4,6-trichlorophenol by activated peroxymonosulfate with sulfur doped copper manganese bimetallic oxides. Chemical Engineering Journal, 417: 128121 doi:10.1016/j.cej.2020.128121

Liu X, Zhou J, Xia Q, Li B, Gao Q, Zhao S, Khan A, Xu A, Li X (2023). Modified birnessite MnO2 as efficient fenton-like catalysts through electron transfer process between the simultaneously surface-activated peroxymonosulfate and pollutants. Journal of Hazardous Materials, 443: 130178 doi:10.1016/j.jhazmat.2022.130178

Tang M, Liu W, Wang Z, Hu Z, Wan J, Peng R (2025). Unexplored role of nanoconfinement in regulating contaminant oxidation pathways for water decontamination: confined energy driving low-carbon route. Chemical Engineering Journal, 507: 160733 doi:10.1016/j.cej.2025.160733

Wang C, Xu S, Liao W, Wang T (2024a). Enhanced sulfamethoxazole degradation using an efficient co-doped MnO2 activator for peroxymonosulfate activation. Desalination and Water Treatment, 317: 100140 doi:10.1016/j.dwt.2024.100140

Wang S, Yuan C, Chen W, Niu Y, Yan Y, Li F, Jiang H (2024b). 3D spherical CuO@g-C3N4 composites activating peroxymonosulfate for high efficient degradation of 2,4,6-trichlorophenol: the mechanism of 1O2 generation. Chemical Engineering Journal, 480: 148050 doi:10.1016/j.cej.2023.148050

Xiong W, Hu F, Liu Y, Nie G, Xiao L (2022). Core-shell FeMn@NG derived from cellulose supported prussian blue analogs for peroxymonosulfate activation: non-radical mechanism and ultra-low metal leaching. Journal of Environmental Chemical Engineering, 10(5): 108523 doi:10.1016/j.jece.2022.108523

Xu R, Ren H, Chi T, Zheng Y, Xie Y, Tian J, Chen L (2022). Ozone oxidation of 2,4,6-TCP in the presence of halide ions: kinetics, degradation pathways and toxicity evaluation. Chemosphere, 288: 132343 doi:10.1016/j.chemosphere.2021.132343

Yazdanbakhsh A, Eslami A, Moussavi G, Rafiee M, Sheikhmohammadi A (2018). Photo-assisted degradation of 2, 4, 6-trichlorophenol by an advanced reduction process based on sulfite anion radical: degradation, dechlorination and mineralization. Chemosphere, 191: 156–165 doi:10.1016/j.chemosphere.2017.10.023